Early detonation by sprouted mossy fibers enables aberrant dentate network activity

William D. Hendricks[a,b], Gary L. Westbrook[c], and Eric Schnell[b,d,1]

[a]Neuroscience Graduate Program, Vollum Institute, Oregon Health & Science University, Portland, OR 97239; [b]Department of Anesthesiology and Perioperative Medicine; Oregon Health & Science University, Portland, OR 97239; [c]Vollum Institute, Oregon Health & Science University, Portland, OR 97239; and [d]Veterans Affairs Portland Health Care System, Portland, OR 97239

Edited by Roger A. Nicoll, University of California, San Francisco, CA, and approved April 16, 2019 (received for review December 13, 2018)

In temporal lobe epilepsy, sprouting of hippocampal mossy fiber axons onto dentate granule cell dendrites creates a recurrent excitatory network. However, unlike mossy fibers projecting to CA3, sprouted mossy fiber synapses depress upon repetitive activation. Thus, despite their proximal location, relatively large presynaptic terminals, and ability to excite target neurons, the impact of sprouted mossy fiber synapses on hippocampal hyperexcitability is unclear. We find that despite their short-term depression, single episodes of sprouted mossy fiber activation in hippocampal slices initiated bursts of recurrent polysynaptic excitation. Consistent with a contribution to network hyperexcitability, optogenetic activation of sprouted mossy fibers reliably triggered action potential firing in postsynaptic dentate granule cells after single light pulses. This pattern resulted in a shift in network recruitment dynamics to an "early detonation" mode and an increased probability of release compared with mossy fiber synapses in CA3. A lack of tonic adenosine-mediated inhibition contributed to the higher probability of glutamate release, thus facilitating reverberant circuit activity.

epilepsy | mossy fiber | sprouting | seizure | adenosine

Mossy fibers contacting CA3 pyramidal cells have a low probability of release (P_r) but show profound short-term facilitation (1). These "conditional detonator" synapses strongly drive postsynaptic cell firing during repetitive activation (2). In experimental and human epilepsy, mossy fiber axons sprout collaterals onto the proximal dendrites of other dentate granule cells (3–6), where conditional detonation could be highly epileptogenic. However, sprouted mossy fibers are smaller than mossy fiber synapses in CA3 (7–9) and rapidly depress during repetitive activation (8), suggesting the extent with which they drive seizure activity could be limited (10).

Despite multiple lines of evidence demonstrating de novo recurrent connections in rodent models of epilepsy, the impact of mossy fiber sprouting on circuit dynamics remains uncertain (11–14). Sprouted mossy fibers are absent under nonpathological conditions, and the formation of novel recurrent connections capable of activating postsynaptic granule cells (15) could induce runaway excitation, particularly if they robustly activate the typically quiescent dentate network. Although increased dentate excitation occurs in temporal lobe epilepsy (16, 17), the challenge of isolating and selectively stimulating sprouted mossy fibers has severely hampered studies that directly examine sprouted mossy fiber synapses (15) and an understanding of how the activation of these fibers might contribute to epileptiform activity.

Here, we selectively activated sprouted mossy fiber axons with optogenetics to determine their influence on postsynaptic granule cell firing and dentate gyrus activity. We find that sprouted mossy fibers reliably drive postsynaptic action potential (AP) firing in dentate granule cells and initiate recurrent circuit activity even in the absence of manipulations to increase excitability. This effect is mediated by increased release probability at these synapses, attributed to a lack of tonic adenosine signaling in the inner molecular layer of the dentate gyrus. The increased P_r allows sprouted mossy fiber activation to reliably recruit postsynaptic circuits, as primed network "spark plugs."

Results

As the functional contribution of mossy fiber sprouting to epileptogenesis remains controversial (10–13), we combined the pilocarpine model of temporal lobe epilepsy with electrophysiology to directly examine the contribution of sprouted mossy fiber activation to epileptiform activity, as this model reliably induces dense mossy fiber sprouting (see *Methods*, also see ref. 8). To isolate sprouted mossy fibers from other granule cell inputs, we used DcxCre::ChR2 mice (18) to selectively label neonatally born granule cells with channelrhodopsin2 (ChR2) (Fig. 1*A*). We then prepared acute mouse hippocampal slices and optogenetically activated sprouted mossy fibers while recording from ChR2-negative (unlabeled) granule cells (Fig. 1 *B* and *C* and *SI Appendix*, Fig. S1; also see ref. 8). Optogenetic activation of sprouted mossy fibers evoked EPSCs in dentate granule cells only in slices from pilocarpine-treated mice (Fig. 1 *D* and *E*; also see ref. 8). Postsynaptic cells, filled with Alexa Fluor 568 dye during recordings, did not have hilar basal dendrites (0 of 32 cells; Fig. 1*C*), indicating that LED-evoked responses originated from recurrent (sprouted mossy fiber) synaptic inputs.

In addition to monosynaptic sprouted mossy fiber–granule cell (smf-GC) EPSCs, we frequently observed LED-evoked epileptiform activity following single light pulses (Fig. 1*D*, *Right*). Responses identified as bursts had, on average, 2.3 ± 0.3 EPSCs during a burst (n = 13 cells). These bursts were not a result of altered intrinsic properties compared with cells with single or no evoked recurrent EPSCs (R_i, input resistance: cells without bursts, 610 ± 47 MΩ, n = 19 cells; cells with bursts, 527 ± 77 MΩ, n = 13 cells; unpaired t test, t_{30} = 0.9711, P = 0.3392; C_m, cell

Significance

Sprouted mossy fibers are one of the hallmark histopathological findings in experimental and human temporal lobe epilepsy. These fibers form recurrent excitatory synapses onto other dentate granule cells that display profound short-term depression. Here, however, we show that although these sprouted mossy fibers weaken substantially during repetitive activation, their initial high probability of glutamate release can activate reverberant network activity. Furthermore, we find that a lack of tonic adenosine inhibition enables this high probability of release and, consequently, recurrent network activity.

Author contributions: W.D.H., G.L.W., and E.S. designed research; W.D.H. performed research; W.D.H. analyzed data; and W.D.H. and E.S. wrote the paper.

The authors declare no conflict of interest.

This article is a PNAS Direct Submission.

Published under the PNAS license.

[1]To whom correspondence should be addressed. Email: schneler@ohsu.edu.

This article contains supporting information online at www.pnas.org/lookup/suppl/doi:10.1073/pnas.1821227116/-/DCSupplemental.

Published online May 13, 2019.

Downloaded at Palestinian Territory, occupied on December 14, 2021

www.manaraa.com

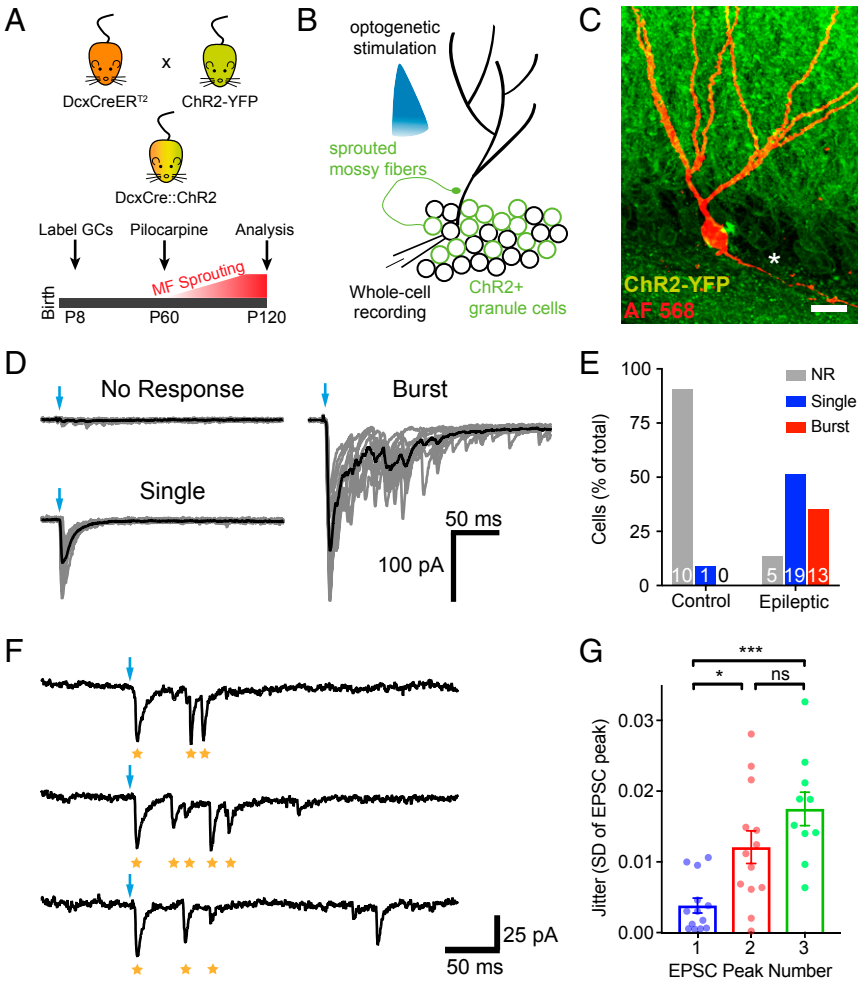

Fig. 1. Stimulation of sprouted mossy fibers triggers spiking in postsynaptic dentate granule cells and recurrent network activity. (*A*) Experimental design for granule cell labeling and induction of epileptic mossy fiber sprouting. DcxCreER^{T2} mice were bred with conditional ChR2-YFP (Ai32) reporter mice (*Upper*) and given TAM at P8 to turn on reporter gene expression (*Lower*). At 2 mo old (P60), mice were given pilocarpine to induce seizures and mossy fiber sprouting or kept as controls. All analysis was at P120. (*B*) Whole-cell recordings were performed on ChR2-negative dentate granule cells (black circles) and sprouted mossy fiber axons were stimulated with blue (470 nm) LED light delivered through the objective. (*C*) Representative confocal image of a recorded granule cell filled with Alexa Fluor 568 (50 μM) during whole-cell recording (levels and gamma adjusted for clarity). Asterisk designates mossy fiber axon; no basal dendrites were present. (Scale bar: 10 μm.) (*D*) Example traces from cells with no response (*Upper Left*), single EPSCs (*Lower Left*), and epileptiform bursts (*Right*) after single optogenetic stimulation of ChR2^{+} granule cells (blue arrows). Scale bar at *Right* applies to all traces. (*E*) Frequency of cells with no response (NR), single EPSCs (Single), and EPSC bursts (Burst) in control and epileptic mice. Number of cells in each category are listed on the graph. (*F*) Three consecutive traces taken from a cell with EPSC bursts. Optogenetic stimulation (blue arrow) evoked an initial EPSC (likely monosynaptic) followed by variably timed burst EPSCs. Gold stars designate detected EPSCs. EPSCs occurring later in the sweep were not counted, as they did not occur within our 100-ms poststimulus timeframe to be considered part of the burst. (*G*) Jitter (trial to trial variability of EPSC onsets, as SD) taken from the first three peaks in an EPSC burst is increased after the first EPSC peak (EPSC jitter: Peak 1, $n = 13$; Peak 2, $n = 13$; Peak 3, $n = 10$; one-way ANOVA, $F_{2,33} = 12.0$, $P = 0.0001$; Tukey's test, Peak 1 vs. Peak 2, $P = 0.0105$; Peak 1 vs. Peak 3, $P < 0.0001$; Peak 2 vs. Peak 3, $P = 0.1544$). High variability in second and third EPSC peaks within a burst suggest that they result from polysynaptic activity. Summary data presented as mean ± SEM. *$P < 0.05$; ***$P < 0.001$; ns, not significant.

capacitance: cells without bursts, 51.5 ± 3.8 pF, $n = 19$ cells; cells with bursts, 46.8 ± 3.8, $n = 13$ cells; unpaired t test, $t_{30} = 0.8302$, $P = 0.4130$). Optogenetic stimulation only elicited single spikes in ChR2-expressing granule cells (number of APs per 1 ms of light pulse: 0.98 ± 0.09, $n = 5$ cells), indicating that sprouted mossy fiber activation initiated recurrent activity. Consistent with polysynaptic activation, EPSC peaks during bursts (EPSC peaks 2–3) had high jitter (Fig. 1 *F* and *G*). One possible source of these bursts is through the activation of additional populations of granule cells with their own sprouted mossy fibers, if sprouted mossy fibers could effectively drive postsynaptic firing.

Unlike healthy mossy fiber–CA3 synapses (1) that are described as conditional detonators, sprouted mossy fiber synapses exhibit profound frequency-dependent short-term depression (*SI Appendix*, Fig. S2, see also ref. 8), which may limit their ability to drive postsynaptic firing (10). Thus, we compared patterns of synaptically evoked spike generation in postsynaptic target cells at these two different synapses using a short 10-Hz train of optogenetic stimulation. In striking contrast to synaptic facilitation and delayed CA3 pyramidal cell spike generation at mf-CA3 synapses, 10-Hz stimulation of sprouted mossy fiber synapses induced postsynaptic spikes only at the beginning of the train (Fig. 2). Importantly, this firing pattern did not result from a failure to activate sprouted mossy fibers in epileptic brains, as these fibers maintain AP fidelity throughout optogenetic trains (*SI Appendix*, Fig. S1). Thus, the failure to maintain postsynaptic activation resulted instead from reduced glutamate release later in the train, consistent with short-term synaptic depression at

Downloaded at Palestinian Territory, occupied on December 14, 2021
www.manaraa.com

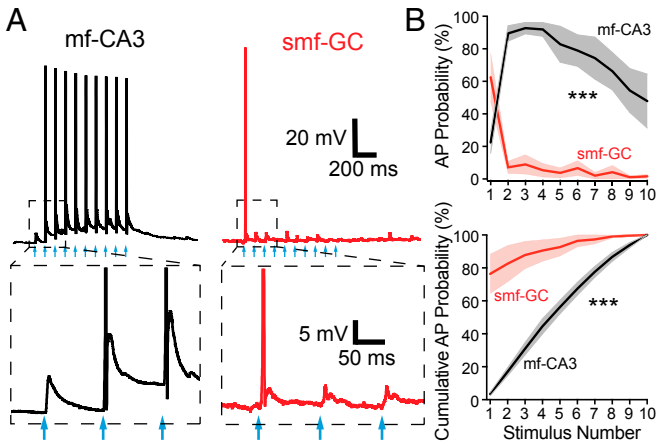

Fig. 2. Sprouted mossy fiber activation drives postsynaptic granule cell firing early during brief trains. (*A*) Representative current clamp recordings during mf-CA3 (black trace) and smf-GC (red trace) activation by 10-Hz, 10-pulse LED trains (blue arrows). Dashed boxes represent insets (below) highlighting facilitation of mf-CA3 EPSPs (*Left*) and depression of smf-GC EPSPs (*Right*). (*B*) AP probability (*Upper*) is shifted to the first stimulus after smf-GC activation relative to mf-CA3 activation (mf-CA3, $n = 6$ cells; smf-GC, $n = 8$ cells, two-way RM ANOVA, $F_{1,12} = 85.68$, $P < 0.0001$; Sidak's multiple comparisons test, Stimulus 1, $P = 0.0048$, Stimuli 2–9, all $P < 0.0001$, Stimulus 10, $P = 0.0006$). Cumulative AP distribution (*Lower*) was also significantly shifted (Kolmogorov–Smirnov test, $P = 0.0006$). Summary data presented as mean ± SEM ***$P < 0.001$.

these synapses (8). Despite this depression, however, single pulses triggered circuit activation sufficient to recruit additional recurrent networks (Fig. 1*D*).

Both the frequency-dependent short-term depression and the robust initial recruitment of postsynaptic cell firing during recurrent activation (Fig. 2*B*) could result from a high initial P_r at sprouted mossy fiber synapses. To directly test for increased P_r, we measured use-dependent MK-801 block kinetics during activation of both types of mossy fiber synapses. Optogenetically evoked NMDAR-mediated synaptic currents were isolated by voltage-clamping granule cells to −70 mV in Mg^{2+}-free ACSF, in the presence of NBQX (10 μM) and SR95531 (10 μM) to block AMPA and $GABA_A$ receptors, respectively. After baseline EPSC recording, LED stimulation was paused for 10 min while MK-801 (40 μM) was washed onto the slice and allowed to equilibrate. Upon resuming LED stimulation (0.05 Hz), MK-801 progressively blocked NMDAR-EPSCs from smf-GC and mf-CA3 synapses (Fig. 3*A*). The rate of block was faster for sprouted mossy fiber synapses (Fig. 3*B*), indicating a higher P_r. Interestingly, MK-801 block rate at smf-GC synapses was better fit by a double-exponential decay model (Fig. 3*C*), whereas at mf-CA3 synapses, a single exponential model was sufficient, suggesting increased synaptic heterogeneity at sprouted mossy fiber synapses (19). Overall, the increased P_r at sprouted mossy fiber synapses likely contributes to target granule cell firing and, therefore, the spread of recurrent excitation in epileptic brains.

Extracellular adenosine inhibits neurotransmitter release at mossy fiber synapses in CA3 via A1-type adenosine receptors (A_1Rs) located on mossy fiber terminals. This tonic activation of presynaptic A_1Rs contributes to the profound short-term plasticity at these synapses (20, 21). As altered adenosine metabolism may be a contributing factor in epileptogenesis (22–24), we posited that sprouted mossy fibers might manifest an increased P_r due to a reduction in A_1R-mediated inhibition. To measure tonic A_1R-mediated inhibition of sprouted mossy fibers in epileptic mice, we washed on the selective high-affinity A_1R antagonist, 8-Cyclopentyl-1,3-dipropylxanthine (DPCPX, 200 nM), while recording sprouted mossy fiber-mediated responses. In contrast to the enhancement of synaptic transmission at healthy mf-CA3 synapses (Fig. 4 *A* and *B*, also see ref. 20), DPCPX had no effect on sprouted mossy fiber EPSCs (Fig. 4 *A* and *B*), indicating a lack of tonic A_1R signaling. The DPCPX-induced increase in EPSC amplitudes at mf-CA3 synapses coincided with decreased PPR (paired-pulse ratio, P_2/P_1: pre-DPCPX, 2.36 ± 0.37; post-DPCPX, 1.37 ± 0.12, $n = 6$ cells; paired t test, $t_5 = 3.408$ $P = 0.0191$), as expected for a presynaptic effect on A_1Rs.

To determine whether the lack of tonic A_1R-mediated inhibition at sprouted mossy fiber synapses resulted from an absence of presynaptic adenosine receptors, we washed on the selective A_1R agonist, 2-Chloro-N^6-cyclopentyladenosine (CCPA, 1 μM). CCPA reduced sprouted mossy fiber EPSCs (Fig. 4 *C* and *D*) and increased paired-pulse facilitation (*SI Appendix*, Fig. S3). Thus, A_1Rs were present and functional on sprouted mossy fiber terminals, indicating that the lack of tonic A_1R modulation was due to a reduced extracellular adenosine concentration. CCPA decreased the probability of release at sprouted mossy fiber synapses, but it did not restore frequency facilitation (*SI Appendix*, Fig. S4), suggesting that the molecular mechanisms underlying synaptic facilitation at mossy fiber terminals cannot be restored solely by increasing A_1R activation.

Finally, to test whether reduced A_1R activation and increased P_r at sprouted mossy fiber synapses contributes to recurrent circuit activation, we examined the effect of A_1R activation using hippocampal slices from epileptic mice. When applied to slices demonstrating EPSC bursts after sprouted mossy fiber activation, the A_1R agonist CCPA reduced recurrent EPSCs (Fig. 4 *E* and *F*) as well as the charge transfer carried by polysynaptic bursts (% of total charge transfer carried by burst: pre-CCPA, 36.5 ± 5.1%, post-CCPA 22.8 ± 4.4%, $n = 5$ cells, paired t test, $t_4 = 3.497$, $P = 0.0250$). Together, these data indicate that

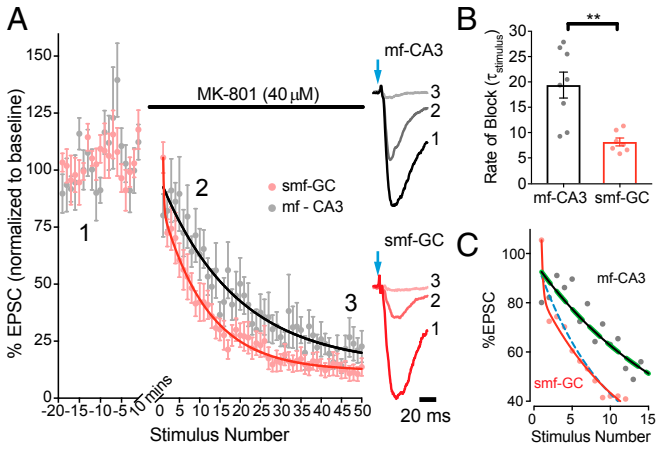

Fig. 3. Elevated probability of release at sprouted mossy fiber synapses. (*A*) P_r was measured from the kinetics of use-dependent MK-801 block of NMDAR-mediated EPSCs during 0.05-Hz LED stimulation. Averaged and normalized responses (*Left*) are plotted before and after bath application of MK-801 (40 μM; mf-CA3, $n = 8$; smf-GC, $n = 7$). Representative, peak-scaled NMDAR EPSC averages (*Right*) were taken during baseline, shortly after resuming LED stimulation, and at the end of the experiment, numbered 1, 2, 3, respectively. (*B*) Average rate of MK-801 block measured in individual cells. MK-801 rate of block was significantly faster at sprouted mossy fiber synapses (unpaired t test, $t_{13} = 3.942$, $P = 0.0017$), indicating higher P_r. (*C*) Same as in *A*, but only showing the first 15 sweeps in MK-801. Single (solid lines) and double (dashed lines) exponential fits are plotted for smf-GC (red and blue) and mf-CA3 (black and green). Sprouted mossy fibers are better fit by double exponential decays (extra sum of squares F test, $F_{2,395} = 5.07$, $P = 0.0067$), whereas mf-CA3 synapses are fit identically by single and double models. All data are presented as mean ± SEM. **$P < 0.01$.

Downloaded at Palestinian Territory, occupied on December 14, 2021
www.manaraa.com

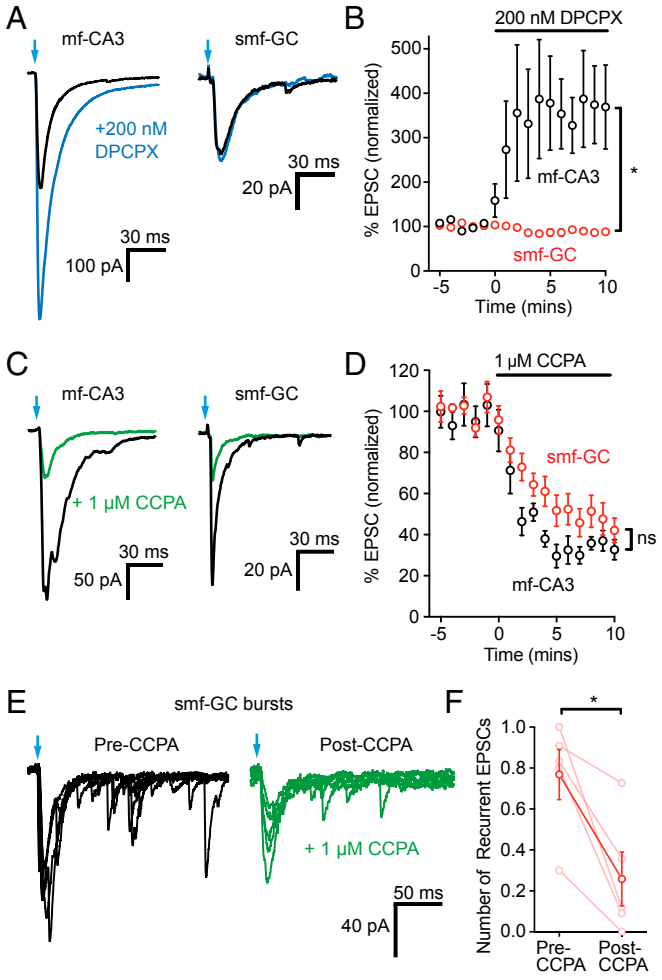

Fig. 4. Lack of tonic adenosine contributes to increased release probability and polysynaptic activity. (*A*) mf-CA3 (*Left*) and smf-GC (*Right*) EPSCs before (black traces) and after (blue traces) washing on the adenosine 1a receptor (A_1R) antagonist DPCPX (200 nM). Bath application of DPCPX facilitates mf-CA3 EPSCs ($n = 8$ cells, paired t test, $t_7 = 5.77$, $P = 0.0007$) but has no effect on EPSC amplitudes at smf-GC synapses ($n = 5$ cells, paired t test, $t_4 = 1.39$, $P = 0.2364$). (*B*) Normalized EPSC amplitudes of mf-CA3 (black, $n = 8$ cells) and smf-GC (red, $n = 5$ cells) responses before and during DPCPX administration (unpaired t test, $t_{11} = 3.63$ $P = 0.0040$). (*C*) The A_1R agonist CCPA (1 μM) inhibits both mf-CA3 (*Left*) and smf-GC (*Right*) EPSCs similarly (baseline, black example traces; CCPA, green traces). (*D*) Normalized mf-CA3 (black) and smf-GC (red) EPSC amplitudes during CCPA application, demonstrating intact A_1R responses at both synapses (mf-CA3, $n = 7$ cells, smf-GC, $n = 12$ cells; unpaired t test, $t_{17} = 1.08$, $P = 0.2954$). (*E*) Adenosine A_1R agonism inhibits recurrent polysynaptic network activity evoked by single-pulse optogenetic stimulation of sprouted mossy fibers. Examples are five consecutive EPSC traces overlaid from the same cell, pre- and post-CCPA (black and green, respectively). (*F*) Quantification of EPSC burst inhibition by CCPA at smf-GC synapses. CCPA (1 μM) reduces the mean number of recurrent EPSCs during a burst (number of recurrent EPSCs per epoch, $n = 5$ cells, $t_4 = 3.963$, $P = 0.0166$). Summary data presented as mean ± SEM. *$P < 0.05$; ns, not significant.

reduced A_1R activation at granule cell outputs contributes to hyperexcitability in the dentate gyrus in epileptic brains.

Discussion

Here, we show that sprouted mossy fibers can trigger reverberating network activity despite their profound short-term depression. This recurrent network activation is enabled by a high probability of release, resulting in early detonation of postsynaptic cells. Moreover, this is due, at least in part, to the lack of tonic adenosine inhibition at sprouted mossy fiber synapses in the inner molecular layer.

The retrograde sprouting of mossy fibers is common to both animal models of epilepsy and human patients with temporal lobe epilepsy (25), yet the functional impact of these recurrent synapses is not well understood (10, 11). We demonstrate that single optogenetic stimulation of these fibers can produce bursts of recurrent EPSCs, suggesting that sprouted mossy fibers effectively recruit the local network. This observation is consistent with paired granule cell recordings from epileptic mice (15), which suggest that sprouted mossy fibers form recurrent excitatory connections capable of driving postsynaptic cell spiking. Critically, we find that sprouted mossy fibers can potently trigger granule cell AP firing with single coordinated release events, which could lead to bursts as successive rounds of sprouted mossy fibers are activated through additional granule cell firing.

The functional effects of sprouted mossy fibers on dentate excitability in ex vivo slice preparations has been difficult to determine, as it sometimes requires modulation of the extracellular environment to reduce the masking effects of inhibition (16, 26–29). This suggests that although the state of the epileptic dentate network may be relatively stable (30), subtle changes in external K^+ concentration (27, 28), inhibition (16, 28), or adenosine (23, 31, 32) could shift the network to a more unstable, hyperexcitable state, during which sprouted mossy fibers can readily trigger epileptiform activity. The absence of tonic adenosine signaling appears to be intrinsic to epileptic slices, recorded using standard solutions. However, it remains likely that changes in adenosine-mediated signaling may serve as another conditional factor in vivo, which might vary over time and contribute to the occurrence (or avoidance) of seizure activity, given the presence of functional adenosine receptors at these synapses.

All EPSC bursts were self-limited, which may be a manifestation of the strong short-term depression of the smf-GC synapse (8, 15). This also helps explain prior indirect observations made using extracellular retrograde stimulation of mossy fibers, which caused self-limited episodes of granule cell population spiking in slices from epileptic rats (33). By using direct optogenetic stimulation of sprouted fibers, we demonstrate sprouted mossy fibers can indeed drive granule cell firing even with inhibition intact and low (3 mM) external K^+ concentrations. We recognize that the conclusions that can be made while using optogenetic stimulation in an acute slice preparation in regards to seizure activity in vivo are limited, primarily due to the isolation of slices from other brain networks and the cerebral extracellular environment and synchronized activation of sprouted terminals. However, our ability to robustly trigger recurrent network activation suggests that recurrent networks are widespread even within our 300-μm brain slices, and that recurrent interconnectivity might be even more extreme within the intact brain.

The increased P_r at sprouted mossy fibers provides a reasonable mechanism that could enable sprouted mossy fibers to act as spark plugs to hyperactivate local dentate gyrus networks. Our direct comparisons of P_r between smf-GC and mf-CA3 synapses are consistent with previous data demonstrating a larger success rate at individual smf-GC connections (0.35) (15) than the prior estimate of P_r at mf-CA3 synapses of 0.2–0.28 (34). We propose that the increased P_r at these sprouted synapses is, at least in part, due to reduced tonic inhibition by adenosine at the smf-GC synapse.

Although we did observe an increase in PPR with CCPA (suggesting that it lowered P_r), our observation that 1-Hz facilitation was not restored by adenosine agonism was somewhat surprising, given the extent to which A1R antagonism occludes frequency facilitation at mf-CA3 synapses in healthy brains (20). This indicates that tonic adenosine alone is unlikely to be the only mechanism controlling short-term plasticity in the smf-GC synapse. This is supported by the previous observation that

NEUROSCIENCE
Downloaded at Palestinian Territory, occupied on December 14, 2021
www.manaraa.com

healthy mossy fiber synapses still express small but significant frequency-dependent facilitation even in the presence of A1R blockade or A1R gene knockout (20). Thus, the short-term depression remaining at smf-GC synapses even in the presence of CCPA could be due to other changes in neuromodulatory tone in the epileptic dentate gyrus or altered expression of specific components of the release machinery required for facilitation (35, 36). Even in healthy brains, the expression of frequency-dependent facilitation by mossy fibers is target-specific (37) and, thus, the remaining differences may also partly derive from differences in the postsynaptic complement between granule cells and CA3 pyramidal cells.

Does the lack of tonic adenosine in the dentate gyrus contribute to seizure activity in epilepsy? Although systemic or local injections of A_1R agonists can reduce the severity of seizures (31, 32), adenosine has broad inhibitory effects throughout the brain. Here, the absence of tonic adenosine signaling at these synapses heightens the excitability of dentate gyrus circuitry, which was reduced by pharmacological A_1R activation (Fig. 4). As the granule cell network is implicated in spontaneous seizures in vivo (38), restoration or augmentation of extracellular adenosine could reduce recurrent circuit dynamics in the dentate gyrus and provide one mechanism for the observed in vivo effects of adenosine (31, 32). Thus, although seizure activity in epileptic brains likely results from multiple hyperexcitable circuit elements, the lack of tonic adenosine signaling in the dentate gyrus shifts sprouted mossy fiber synapses from "conditional detonators" to "early detonators," which could contribute to the initiation of generalized seizures.

Methods

Animals. All experiments were carried out in accordance with local, state, and federal guidelines, and protocols were approved by Oregon Health & Science University (OHSU) and Veterans Affairs Institutional Animal Care and Use Committees. Housing was provided by OHSU's Department of Comparative Medicine vivarium accredited by the Association for Assessment and Accreditation of Laboratory Animals. To generate DcxCre::ChR2 mice, homozygous *doublecortin-CreER^{T2}* (line F18; RRID:MGI:5438982) mice were bred with homozygous *Gt(ROSA)26Sor$^{tm32(CAG-COP4*H134R/EYFP)Hze}$* (Ai32; RRID:IMSR_JAX:012569) and used as described (8, 18). Briefly, Cre-mediated combination was induced by tamoxifen (TAM) at postnatal day (P)8 (two injections, 12 h apart, 20 mg/kg in corn oil, i.p.), to permanently label neonatally generated granule cells with ChR2-eYFP in DcxCre::ChR2 heterozygous mice. Status epilepticus was induced in 2-mo-old male mice with pilocarpine (325 mg/kg i.p.; Cayman Chemicals) after pretreating with an i.p. injection of scopolamine methyl bromide (Sigma-Aldrich). Seizures were graded on the modified Racine Scale (39); status epilepticus (SE) was defined when a mouse had three or more Racine Grade 3 seizures, followed by continuous grade 2 seizing. Following 2 h of SE, seizures were terminated with diazepam (10 mg/kg i.p.; Hospira, Inc.) and given soft food and i.p. injections of 5% glucose in 0.45% normal saline to aid in recovery. Mice that did not develop SE were humanely killed by carbon dioxide inhalation and cervical dislocation and excluded from further analysis. These criteria reliably produce dense mossy fiber sprouting as measured by ZnT3 staining in the IML, and a high density of sprouted mossy fibers originating from granule cells specifically labeled at this timepoint (8). A total of 23 healthy control mice and 19 pilocarpine-treated mice were used in this study.

Slice Physiology. Acute brain slices for ex vivo electrophysiology were prepared as described (8). In brief, 4-mo-old male DcxCre::ChR2 mice were anesthetized with 4% isoflurane, followed by injection of 1.2% avertin (Sigma-Aldrich). Mice were transcardially perfused with 10 mL of ice-cold *N*-methyl-D-glucamine (NMDG)-based cutting solution, containing the following (in mM): 93 NMDG, 30 $NaHCO_3$, 24 glucose, 20 Hepes, 5 Na-ascorbate, 5 *N*-acetyl cysteine, 3 Na-pyruvate, 2.5 KCl, 2 thiourea, 1.2 NaH_2PO_4, 10 $MgSO_4$, and 0.5 $CaCl_2$. Mice were rapidly decapitated and 300-μm sagittal slices were prepared with a Leica VT1200S vibratome. This method was chosen to best preserve CA3 pyramidal cell health and mossy fiber axons from these 4-mo-old mice. For some dentate granule cell recordings, the hippocampus was dissected, and 300-μm transverse hippocampal sections were prepared in ice-cold NMDG solution, which allowed us to maximize the number of slices obtained from epileptic animals. We did not observe any physiological differences between the two preparations during granule cell recordings, including the frequency of smf-GC bursts, so these results were combined. Slices from both preparations recovered in warm NMDG cut solution for 15 min followed by standard ACSF at room temperature for 1 h before recording.

Dentate granule cell and CA3 pyramidal cell recordings were obtained with 3–5 MΩ borosilicate glass pipettes filled with internal solution. The Cs^+-based internal solution for voltage-clamp experiments contained the following (in mM): 113 Cs-gluconate, 17.5 CsCl, 10 Hepes, 10 EGTA, 8 NaCl, 2 Mg-ATP, 0.3 Na-GTP, 0.05 Alexa Fluor 568, pH adjusted to 7.3 with CsOH, with a final osmolarity of 295 mOsm; QX-314-Cl (5 mM; Tocris Bioscience) was included to block unclamped APs. The K^+-based internal solution for current-clamp experiments contained the following (in mM): 130 K-gluconate, 20 KCl, 10 Hepes, 4 Mg-ATP, 0.3 Na-GTP, 0.1 EGTA, 0.05 Alexa Fluor 568, pH adjusted to 7.2 KOH, with a final osmolarity of 295 mOsm. Granule cells and CA3 pyramidal cells were identified with infrared differential interference contrast microscopy on an Olympus BX-51WI microscope. Whole-cell recordings were obtained by making high-resistance seals (>5 GΩ) and applying brief suction. Cells were filled with Alexa Fluor 568 dye to visually confirm cell type and assess for presence of hilar basal dendrites. Series resistance was uncompensated, and cells with a >30% change in series resistance were excluded from analysis. Liquid junction potential was 8 mV and was uncorrected. For current-clamp recordings, minimal negative current was injected, if necessary, to maintain a resting potential of −70 mV in dentate granule cells and CA3 pyramidal cells.

Pulses of blue LED-powered (Thorlabs) light (1 ms, 470 nm, 8 mW/cm^2, 0.05 Hz) were delivered through a 40x water immersion objective, targeted at the stratum lucidum for CA3 recordings and inner molecular layer for granule cell recordings. Stimulation frequency was modified for various experiments as noted in the text. Signals were amplified with an AxoPatch 200B amplifier (Molecular Devices), low-pass Bessel-filtered at 5 kHz, and digitized and sampled at 10 kHz using a NIDAQ (National Instruments) analog-to-digital board. Data were captured using a custom Igor Pro 8 (Wavemetrics) script and NIDAQmx (National Instruments) plugins. For presentation of EPSCs, a 2-kHz Gaussian filter was applied, post hoc.

Statistical Analysis. Curve fitting and EPSC trace averaging was carried out in Igor Pro 8 (Wavemetrics) using built-in and custom functions, respectively. Epileptiform burst activity (multiple EPSCs to single stimulus) was determined by eye, aided by fitting a single exponential curve to the initial decay and identifying delayed EPSC peaks rising above the decay fit line. Peak detection was implemented in Igor Pro by identifying zero-point crossings of thresholded peaks on the first-order derivative of the EPSC. Charge transfer measurements were implemented with Igor Pro's area function. Additional statistical analysis was performed in Prism 8 (GraphPad). Normality was tested with the Shapiro–Wilk normality test before statistical test selection. Paired and unpaired *t* tests were used for normally distributed datasets; Mann–Whitney and Wilcoxon matched-pairs signed rank test were used for nonparametric datasets. For all experiments, significance was determined by $P < 0.05$ ($*P < 0.05$, $**P < 0.01$, $***P < 0.001$). All summary data are presented as mean ± SEM.

ACKNOWLEDGMENTS. We thank Drs. Zhi-Qi Xiong and Xuewen Cheng (Shanghai Institute for Neuroscience) for providing the DcxCreER^{T2} mouse line and members of the E.S. and G.L.W. laboratories for critical feedback and discussion on the manuscript. Research funding was provided by Department of Veterans Affairs, Veterans Health Administration, Office of Research and Development, Biomedical Laboratory and Development CDA-2 Award 005-10S (to E.S.); Department of Veterans Affairs Merit Review Award I01-BX002949 (to E.S.); Department of Defense Congressionally Directed Medical Research Program Award W81XWH-18-1-0598 (to E.S.); National Institutes of Health (NIH) Grant F31-NS098597 (to W.D.H.); NIH Grant R01-NS080979 (to G.L.W.); and NIH Grant P30-NS061800 (OHSU Advanced Light Microscopy Core). The contents of this manuscript do not represent the views of the US Department of Veterans Affairs or the US government.

1. Nicoll RA, Schmitz D (2005) Synaptic plasticity at hippocampal mossy fibre synapses. *Nat Rev Neurosci* 6:863–876.
2. Vyleta NP, Borges-Merjane C, Jonas P (2016) Plasticity-dependent, full detonation at hippocampal mossy fiber-CA3 pyramidal neuron synapses. *eLife* 5:e17977.
3. Sutula T, He XX, Cavazos J, Scott G (1988) Synaptic reorganization in the hippocampus induced by abnormal functional activity. *Science* 239:1147–1150.
4. Sutula T, Cascino G, Cavazos J, Parada I, Ramirez L (1989) Mossy fiber synaptic reorganization in the epileptic human temporal lobe. *Ann Neurol* 26:321–330.
5. Houser CR, et al. (1990) Altered patterns of dynorphin immunoreactivity suggest mossy fiber reorganization in human hippocampal epilepsy. *J Neurosci* 10:267–282.
6. Okazaki MM, Evenson DA, Nadler JV (1995) Hippocampal mossy fiber sprouting and synapse formation after status epilepticus in rats: Visualization after retrograde transport of biocytin. *J Comp Neurol* 352:515–534.

Downloaded at Palestinian Territory, occupied on December 14, 2021
www.manaraa.com

7. Cavazos JE, Zhang P, Qazi R, Sutula TP (2003) Ultrastructural features of sprouted mossy fiber synapses in kindled and kainic acid-treated rats. *J Comp Neurol* 458:272–292.
8. Hendricks WD, Chen Y, Bensen AL, Westbrook GL, Schnell E (2017) Short-term depression of sprouted mossy fiber synapses from adult-born granule cells. *J Neurosci* 37:5722–5735.
9. Sutula T, et al. (1998) Synaptic and axonal remodeling of mossy fibers in the hilus and supragranular region of the dentate gyrus in kainate-treated rats. *J Comp Neurol* 390:578–594.
10. Smith BN (2017) Sprouted mossy fiber connections of adult-born granule cells: Detonate or fizzle? *Epilepsy Curr* 17:379–380.
11. Buckmaster PS (2014) *Does Mossy Fiber Sprouting Give Rise to the Epileptic State? Issues in Clinical Epileptology: A View from the Bench*, eds Scharfman HE, Buckmaster PS (Springer Netherlands, Dordrecht, The Netherlands), Vol 813, pp 161–168.
12. Longo BM, Mello LEAM (1997) Blockade of pilocarpine- or kainate-induced mossy fiber sprouting by cycloheximide does not prevent subsequent epileptogenesis in rats. *Neurosci Lett* 226:163–166.
13. Longo BM, Mello LEAM (1998) Supragranular mossy fiber sprouting is not necessary for spontaneous seizures in the intrahippocampal kainate model of epilepsy in the rat. *Epilepsy Res* 32:172–182.
14. Mello LE, et al. (1993) Circuit mechanisms of seizures in the pilocarpine model of chronic epilepsy: Cell loss and mossy fiber sprouting. *Epilepsia* 34:985–995.
15. Scharfman HE, Sollas AL, Berger RE, Goodman JH (2003) Electrophysiological evidence of monosynaptic excitatory transmission between granule cells after seizure-induced mossy fiber sprouting. *J Neurophysiol* 90:2536–2547.
16. Cronin J, Obenaus A, Houser CR, Dudek FE (1992) Electrophysiology of dentate granule cells after kainate-induced synaptic reorganization of the mossy fibers. *Brain Res* 573:305–310.
17. Wuarin JP, Dudek FE (2001) Excitatory synaptic input to granule cells increases with time after kainate treatment. *J Neurophysiol* 85:1067–1077.
18. Cheng X, et al. (2011) Pulse labeling and long-term tracing of newborn neurons in the adult subgranular zone. *Cell Res* 21:338–349.
19. Rosenmund C, Clements JD, Westbrook GL (1993) Nonuniform probability of glutamate release at a hippocampal synapse. *Science* 262:754–757.
20. Moore KA, Nicoll RA, Schmitz D (2003) Adenosine gates synaptic plasticity at hippocampal mossy fiber synapses. *Proc Natl Acad Sci USA* 100:14397–14402.
21. Fedele DE, et al. (2005) Astrogliosis in epilepsy leads to overexpression of adenosine kinase, resulting in seizure aggravation. *Brain* 128:2383–2395.
22. Boison D (2008) The adenosine kinase hypothesis of epileptogenesis. *Prog Neurobiol* 84:249–262.
23. Sandau US, et al. (2016) Adenosine kinase deficiency in the brain results in maladaptive synaptic plasticity. *J Neurosci* 36:12117–12128.
24. Williams-Karnesky RL, et al. (2013) Epigenetic changes induced by adenosine augmentation therapy prevent epileptogenesis. *J Clin Invest* 123:3552–3563.
25. Buckmaster PS (2012) Mossy fiber sprouting in the dentate gyrus. *Jasper's Basic Mechanisms of the Epilepsies*, eds Noebels JL, Avoli M, Rogawski MA, Olsen RW, Delgado-Escueta AV (Natl Center Biotechnol Inf, Bethesda), p 29.
26. Sutula TP, Dudek FE (2007) Unmasking recurrent excitation generated by mossy fiber sprouting in the epileptic dentate gyrus: An emergent property of a complex system. *Prog Brain Res* 163:541–563.
27. Hardison JL, Okazaki MM, Nadler JV (2000) Modest increase in extracellular potassium unmasks effect of recurrent mossy fiber growth. *J Neurophysiol* 84:2380–2389.
28. Patrylo PR, Dudek FE (1998) Physiological unmasking of new glutamatergic pathways in the dentate gyrus of hippocampal slices from kainate-induced epileptic rats. *J Neurophysiol* 79:418–429.
29. Wuarin JP, Dudek FE (1996) Electrographic seizures and new recurrent excitatory circuits in the dentate gyrus of hippocampal slices from kainate-treated epileptic rats. *J Neurosci* 16:4438–4448.
30. Santhakumar V, Aradi I, Soltesz I (2005) Role of mossy fiber sprouting and mossy cell loss in hyperexcitability: A network model of the dentate gyrus incorporating cell types and axonal topography. *J Neurophysiol* 93:437–453.
31. Amorim BO, et al. (2016) Effects of A1 receptor agonist/antagonist on spontaneous seizures in pilocarpine-induced epileptic rats. *Epilepsy Behav* 61:168–173.
32. Gouder N, Fritschy JM, Boison D (2003) Seizure suppression by adenosine A1 receptor activation in a mouse model of pharmacoresistant epilepsy. *Epilepsia* 44:877–885.
33. Tauck DL, Nadler JV (1985) Evidence of functional mossy fiber sprouting in hippocampal formation of kainic acid-treated rats. *J Neurosci* 5:1016–1022.
34. von Kitzing E, Jonas P, Sakmann B (1994) Quantal analysis of excitatory postsynaptic currents at the hippocampal mossy fiber-CA3 pyramidal cell synapse. *Adv Second Messenger Phosphoprotein Res* 29:235–260.
35. Ben-Simon Y, et al. (2015) A combined optogenetic-knockdown strategy reveals a major role of tomosyn in mossy fiber synaptic plasticity. *Cell Rep* 12:396–404.
36. Jackman SL, Turecek J, Belinsky JE, Regehr WG (2016) The calcium sensor synaptotagmin 7 is required for synaptic facilitation. *Nature* 529:88–91.
37. Toth K, Suares G, Lawrence JJ, Philips-Tansey E, McBain CJ (2000) Differential mechanisms of transmission at three types of mossy fiber synapse. *J Neurosci* 20:8279–8289.
38. Zhou QG, et al. (2019) Chemogenetic silencing of hippocampal neurons suppresses epileptic neural circuits. *J Clin Invest* 129:310–323.
39. Shibley H, Smith BN (2002) Pilocarpine-induced status epilepticus results in mossy fiber sprouting and spontaneous seizures in C57BL/6 and CD-1 mice. *Epilepsy Res* 49:109–120.

Downloaded at Palestinian Territory, occupied on December 14, 2021

www.manaraa.com